



# 1 **Particulate-bound alkyl nitrate pollution and formation** 2 **mechanisms in Beijing, China**

3 Jiyuan Yang<sup>1\*</sup>, Guoyang Lei<sup>1\*</sup>, Jinfeng Zhu<sup>1</sup>, Yutong Wu<sup>1</sup>, Chang Liu<sup>1</sup>, Kai Hu<sup>1</sup>,  
4 Junsong Bao<sup>2</sup>, Zitong Zhang<sup>1</sup>, Weili Lin<sup>1</sup> and Jun Jin<sup>1,3</sup>.

5 <sup>1</sup>College of Life and Environmental Sciences, Minzu University of China, Beijing 100081, China

6 <sup>2</sup>State Key Laboratory of Water Environment Simulation, School of Environment, Beijing Normal  
7 University, Beijing, 100875, China

8 <sup>3</sup>Beijing Engineering Research Center of Food Environment and Public Health, Minzu University of  
9 China, Beijing 100081, China

10 \*These authors contributed equally to this work

11 *Correspondence to:* Jun Jin (junjin3799@126.com)

## 12 **Abstract**

13 Fine particulate matter (PM<sub>2.5</sub>) samples were collected between November 2020 and October 2021 at  
14 the Minzu University of China in Beijing and the *n*-alkyl nitrate concentrations in the PM<sub>2.5</sub> samples  
15 were determined to investigate *n*-alkyl nitrate pollution and formation mechanisms. C<sub>9</sub>–C<sub>16</sub> *n*-alkyl  
16 nitrate standards were synthesized and the *n*-alkyl nitrate concentrations in PM<sub>2.5</sub> were determined by  
17 gas chromatography triple quadrupole mass spectrometry. Temporal trends in and correlations between  
18 particulate-bound *n*-alkyl nitrate, ozone, PM<sub>2.5</sub>, and nitrogen dioxide concentrations were investigated  
19 to assess the relationships between particulate-bound *n*-alkyl nitrate concentrations and photochemical  
20 reactions and identify the *n*-alkyl nitrate formation mechanisms. The *n*-alkyl nitrate concentrations in  
21 the PM<sub>2.5</sub> samples were 9.67–2730 pg/m<sup>3</sup>, and the mean was 578 pg/m<sup>3</sup>. The *n*-alkyl nitrate homologue  
22 group concentrations increased as the carbon chain length increased, i.e. long-chain *n*-alkyl nitrates  
23 contributed more than short-chain *n*-alkyl nitrates to the total *n*-alkyl nitrate concentrations in PM<sub>2.5</sub>.  
24 The *n*-alkyl nitrate concentrations clearly varied seasonally and diurnally, the concentrations decreasing  
25 in the order winter > spring > autumn > summer and the mean concentrations being higher at night than  
26 in the day. The particulate-bound *n*-alkyl nitrate and ozone concentrations significantly negatively  
27 correlated despite gas-phase alkyl nitrate and ozone concentrations previously being found to positively  
28 correlate. This indicated that long-chain alkyl nitrates may not be produced during photochemical  
29 reactions. The particulate-bound *n*-alkyl nitrate concentrations followed the same trends as and  
30 significantly positively correlated with the PM<sub>2.5</sub> and nitrogen dioxide concentrations. Nitrogen dioxide  
31 is an important contributor of nitrates in particulate matter. This indicated that particulate-bound *n*-alkyl  
32 nitrates may form through reactions between alkanes and nitrates on particulate matter surfaces.  
33 Particulate-bound *n*-alkyl nitrates are important components of PM<sub>2.5</sub> during haze events and strongly  
34 affect atmospheric visibility. Particulate-bound *n*-alkyl nitrates are secondary pollutants that strongly  
35 influence haze pollution.

## 36 **1 Introduction**

37 Air pollution problems in China are complex but have been alleviated by adjusting the energy structure



38 and controlling pollutant emissions. However, air pollution (caused by frequent sandstorms in spring,  
39 photochemical pollution with ozone and secondary particles forming in summer and autumn, and  
40 serious haze pollution caused by emissions caused by heating buildings in winter) remains a problem in  
41 urban areas in North China. Air quality in China will therefore continue to pose serious challenges for  
42 some time.

43 Photochemical smog and haze are important types of air pollution that affect ambient air quality.  
44 Interactions between photochemical pollution and particulate pollution have become the main foci of  
45 air pollution research (Ma et al., 2012). Nitrogen oxide (NO<sub>x</sub>) emissions have increased by >50% in  
46 the last 30 years (Liu et al., 2013) and NO<sub>x</sub> concentrations in the atmosphere continue to increase as  
47 the number of vehicles increases (Richter et al., 2005; Mijling et al., 2013). More oxidation occurs in  
48 the atmosphere as NO<sub>x</sub> concentrations increase, and the contributions of anthropogenic emissions to  
49 volatile organic compound (VOC) concentrations in the atmosphere are also increasing (Liu et al.,  
50 2020). Challenges caused by synergistic photochemical smog and haze pollution are affecting urban  
51 areas in which background NO<sub>x</sub> concentrations are high and large amounts of anthropogenic VOCs are  
52 emitted. Future improvements in ambient air quality require both photochemical and particulate  
53 pollution to be controlled. Organic nitrates (ONs) formed in the atmosphere from the precursors NO<sub>x</sub>  
54 and VOCs are important atmospheric pollutants.

55 The general term ONs is used for various atmospheric pollutants with the formula RONO<sub>2</sub> and includes  
56 esters containing nitrate groups and polyfunctional derivatives. ONs are important reactive nitrogen  
57 oxides in the environment and are important participants in the atmospheric nitrogen cycle, which  
58 involves various atmospheric sources and sinks of nitrogen oxides that affect regional NO<sub>x</sub> cycles and  
59 balances (Barnes et al., 1993; Chen et al., 1998; Perring et al., 2010). ONs are important secondary air  
60 pollutants and are very important species affecting oxidation in the atmosphere and the formation of  
61 haze (Browne et al., 2012). ONs formation consumes atmospheric oxidants and affects the atmospheric  
62 lifetimes of free radicals, the ozone concentration, and photochemical reactions (Calvert et al., 1987).  
63 Semi-volatile ONs are important sources and components of secondary organic aerosols (SOAs) and  
64 make important contributions to fine particulate matter (PM<sub>2.5</sub>) (Rollins et al., 2012). Controlling  
65 particulate-bound ONs may therefore be key to controlling both PM<sub>2.5</sub> and ozone in the atmosphere.

66 Particulate-bound nitrates are some of the main components of particulate matter in China, particularly  
67 during pollution events, and strongly affects human health, air quality, and the climate at the regional  
68 scale (Zhai et al., 2023). Particulate-bound ONs are important components of particulate nitrates. SOAs  
69 can contribute 30%–77% of the mass of PM<sub>2.5</sub> during a strong atmospheric pollution event.

70 Between 5% and 40% of the mass of organic matter in particulate matter can be ONs (Rollins et al.,  
71 2012; Xu et al., 2015; Sun et al., 2012). ONs have been found to be bound to atmospheric particles in  
72 various size ranges (Garnes et al., 2002), indicating that ONs are widely present in atmospheric  
73 particulate matter. Recent studies of particulate-bound ONs have mainly been focused on biogenic ONs  
74 formed from precursors such as the olefins pinene (Shen et al., 2021; Rindelaub et al., 2015), limonene  
75 (Spittler et al., 2006), monoterpene (Barnes et al., 1990), and isoprene (Rollins et al., 2009; Perring et  
76 al., 2009; Vasquez et al., 2020; Wu et al., 2020) emitted from plants. Less attention has been paid to  
77 particulate-bound ONs that are related to emissions of anthropogenic pollutants.



78 Alkyl nitrates are common ONs. The alkanes that act as precursors for alkyl nitrates have been found to  
79 be some of the main components of anthropogenic VOCs that are widely present in the atmosphere  
80 (Wei et al., 2018; Kang et al., 2018). It has been found that short-chain ( $C_1$ – $C_5$ ) alkyl nitrates are  
81 secondary products of photochemical reactions between alkanes and  $OH\cdot$  radicals in the gas phase  
82 (Jordan et al., 2008; Lim et al., 2009; Perring et al., 2013; Sun et al., 2018), so are associated with  
83 photochemical pollution (Simpson et al., 2006; Wang et al., 2013; Ling et al., 2016). The vapour  
84 pressure decreases as the carbon chain length increases, so long-chain alkyl nitrates tend to enter the  
85 particle phase through gas–particle partitioning and can participate in particulate matter formation and  
86 contribute to haze pollution (Lim et al., 2005; Yee et al., 2012). Few studies of particulate-bound alkyl  
87 nitrates have been performed, Yang et al. developed a gas chromatography triple quadrupole mass  
88 spectrometry (GC-MS/MS) method for determining *n*-alkyl nitrate concentrations and detected *n*-alkyl  
89 nitrates in real  $PM_{2.5}$  samples (Yang et al., 2019). This indicated that *n*-alkyl nitrates can be present in  
90 airborne particulate matter in urban areas. Particulate-bound alkyl nitrates are important contributors to  
91 haze pollution, so it is important to improve our understanding of particulate-bound alkyl nitrate  
92 pollution, temporal variations, and formation mechanisms.

93 In this study, we determined the concentrations of  $C_9$ – $C_{16}$  *n*-alkyl nitrates in  $PM_{2.5}$  samples collected in  
94 Beijing in 2020 and 2021. The aim was to investigate *n*-alkyl nitrate pollution and assess temporal  
95 variations in *n*-alkyl nitrate compositions and concentrations. We also assessed the similarities in  
96 temporal trends in and correlations between the particulate-bound *n*-alkyl nitrate, ozone,  $PM_{2.5}$ , and  
97 nitrogen dioxide ( $NO_2$ ) concentrations to investigate the mechanisms involved in the formation of  
98 particulate-bound alkyl nitrates. The study was performed to improve our understanding of alkyl  
99 nitrates in  $PM_{2.5}$  and improve our ability to control haze pollution.

## 100 **2 Materials and methods**

### 101 **2.1 Sampling period and location**

102 Beijing is a typical densely populated large city in China. The heavy traffic in Beijing means that large  
103 amounts of exhaust gases are emitted by motor vehicles, and this causes serious haze pollution. Large  
104 amounts of anthropogenic *n*-alkanes are emitted to the atmosphere and act as precursors for  
105 particulate-bound alkyl nitrates. Haidian District is a relatively prosperous area in Beijing. Haidian  
106 District is a busy area with high traffic flows and heavy traffic, making it suitable for studying  
107 anthropogenic alkyl nitrates in particulate matter. This study was performed at the Minzu University of  
108 China (116.19° E, 39.57° N) in Haidian District.  $PM_{2.5}$  samples were collected on the roof (about 20 m  
109 above the ground) of the College of Pharmacy at the Minzu University of China. Samples were  
110 collected in November and December 2021 and March, April, July, September, and October 2022.  
111 Separate day and night samples were collected for one week (23rd to 29th) in each of these months.  
112 Each day-time sample was collected from 07:00 to 20:00 and each night-time sample was collected  
113 from 20:30 to 06:30.

### 114 **2.2 Sample collection and pretreatment**

115 Each  $PM_{2.5}$  sample was collected at a flow rate of 16.7 L/min using a TH-16A low flow sampler  
116 (Wuhan Tianhong, Wuhan, China) containing a Whatman QMA quartz fibre filter ( $\varnothing$  47 mm; GE



117 Healthcare Bio-Sciences, Pittsburgh, PA, USA). Before use, the quartz fibre filters were baked at  
118 550 °C for 5 h to remove organic matter. Each sample was wrapped in aluminium foil and stored at  
119 -20 °C.

120 The *n*-alkyl nitrates in a PM<sub>2.5</sub> sample were extracted using an ultrasonic extraction method that was  
121 described in detail in previous publications (Yang et al., 2019; Yang et al., 2023). The filter was cut into  
122 pieces and extracted with 15.0 mL of dichloromethane for 15 min with ultrasonication. The extraction  
123 step was repeated five times and the extracts were combined and evaporated to 2.0 mL using a rotary  
124 evaporator. The extract was then transferred to a 15 mL centrifuge tube and centrifuged at 3000 rpm for  
125 5 min. The supernatant was then evaporated almost to dryness under a stream of high-purity nitrogen  
126 and transferred into 100 µL toluene for instrumental analysis. The sample pretreatment processes were  
127 performed with light excluded to prevent photolysis of nitrates.

### 128 2.3 Synthesis of standards

129 Standards of *n*-alkyl nitrates could not be purchased, so we synthesized C<sub>9</sub>–C<sub>16</sub> *n*-alkyl nitrate standards  
130 by performing substitution reactions involving treating brominated *n*-alkanes with silver nitrate using a  
131 previously published method (Luxenhofer et al., 1994; Luxenhofer et al., 1996; Yang et al., 2019). The  
132 standards were then analysed by GC-MS/MS.

### 133 2.4 Instrumental analysis

134 The *n*-alkyl nitrates (C<sub>9</sub>–C<sub>16</sub>) were qualitatively and quantitatively analysed using a Trace 1310 gas  
135 chromatograph and TSQ 8000 Evo triple quadrupole mass spectrometer (Thermo Fisher Scientific,  
136 Waltham, MA, USA). Separation was achieved using a J&W Scientific DB-5M column (30 m long,  
137 0.25 mm inner diameter, 0.1 µm film thickness; Agilent Technologies, Santa Clara, CA, USA). The  
138 injection volume was 1.0 µL and splitless injection mode was used. The carrier gas was high-purity  
139 helium and the flow rate was 1.0 mL/min. The oven temperature program started at 60 °C, which was  
140 held for 3 min, then increased at 10 °C/min to 280 °C, which was held for 3 min. The triple quadrupole  
141 mass spectrometer was used in electron impact ionization mode. The ion source temperature was  
142 280 °C and the transmission line temperature was 290 °C. The mass spectrometer was used in selected  
143 ion detection mode and *n*-alkyl nitrates were detected by monitoring the characteristic [NO<sub>2</sub>]<sup>+</sup> ion (m/z  
144 46.07) and [CH<sub>2</sub>ONO<sub>2</sub>]<sup>+</sup> ion (m/z 76.07), which were used as the confirmation and quantitation ions.  
145 The GC-MS/MS data were processed and the *n*-alkyl nitrates were quantified using TraceFinder 2.0  
146 software (Thermo Fisher Scientific).

### 147 2.5 Quantitative analysis

148 The *n*-alkyl nitrates were quantified using an external standards method. We used the synthesized  
149 C<sub>9</sub>–C<sub>16</sub> *n*-alkyl nitrates to prepare standard solutions at concentrations of 1000, 100, 50, 20, and 10  
150 ng/mL. A calibration curve was plotted for each analyte with the concentrations of the standards on the  
151 *x*-axis and the GC-MS/MS instrument responses on the *y*-axis. The linear ranges of the standard curves  
152 for the C<sub>9</sub>–C<sub>16</sub> *n*-alkyl nitrate homologues were 10–1000 ng/mL, and the correlation coefficients were  
153 all >0.998. The *n*-alkyl nitrate concentrations in the PM<sub>2.5</sub> sample extracts were quantified using the  
154 calibration curves.



155 **2.6 Quality assurance and control**

156 Method and spiked blanks were extracted with each batch of samples. The *n*-alkyl nitrate  
157 concentrations found in the blank samples were subtracted from the *n*-alkyl nitrate concentrations  
158 found in the samples. The detection and quantification limits of the GC-MS/MS instrument were  
159 defined as the concentrations giving signal-to-noise ratios of 3 and 10, respectively. The instrument  
160 detection limits for the *n*-alkyl nitrates were 1.0–10.0 pg and the method quantification limits were  
161 0.1–1.0 pg/m<sup>3</sup>.

162 The recoveries of the *n*-alkyl nitrates in the PM<sub>2.5</sub> samples were determined by performing spike  
163 recovery experiments, and the recovery was defined as the ratio between the measured and spiked  
164 concentrations. Three parallel spiked blank samples were analysed, and 20 μL of a standard solution  
165 containing each C<sub>9</sub>–C<sub>16</sub> *n*-alkyl nitrate at a concentration of 100 ng/mL was added to each. The spiked  
166 blanks were then treated and analysed using the method described above. The *n*-alkyl nitrate  
167 concentrations in the spiked blank samples were determined by GC-MS/MS and the recoveries were  
168 calculated. The *n*-alkyl nitrate recoveries were 62.6%–95.3% and the relative standard deviation was  
169 2.65%.

170 **2.7 Data analysis**

171 The PM<sub>2.5</sub>, ozone, and NO<sub>2</sub> concentrations were obtained from the China Meteorological  
172 Administration ([www.cma.gov.cn/](http://www.cma.gov.cn/), last access: 31 October 2021). The particulate-bound *n*-alkyl nitrate  
173 concentration data were statistically analysed using SPSS 26.0 software (IBM, Armonk, NY, USA).  
174 Correlations between concentrations of different species were identified by performing Pearson  
175 correlation and Spearman correlation tests (two-tailed), and differences between the concentrations in  
176 different samples were assessed by performing independent sample t-tests, paired sample t-tests, and  
177 one-way ANOVAs.

178 **3 Results and discussion**

179 **3.1 Particulate-bound *n*-alkyl nitrate pollution**

180 **3.1.1 Concentrations and compositions**

181 The C<sub>9</sub>–C<sub>16</sub> *n*-alkyl nitrates were detected in the PM<sub>2.5</sub> samples collected during day and night in all of  
182 the seasons, and the concentrations are shown in Figure 1. The concentration ranges, mean  
183 concentrations, and detection rates for the different homologues are shown in Table 1.

184 The C<sub>9</sub> and C<sub>10</sub> *n*-alkyl nitrate detection rates were <50%, the C<sub>11</sub> *n*-alkyl nitrate detection rate was  
185 ~70%, and the C<sub>12</sub>–C<sub>16</sub> *n*-alkyl nitrate detection rates were ~90%. The particulate-bound *n*-alkyl nitrate  
186 detection rates generally increased as the carbon chain length increased. These results indicated that  
187 particulate-bound *n*-alkyl nitrates are widely present in airborne particulate matter in Beijing and that  
188 long chain *n*-alkyl nitrates are more abundant than short chain *n*-alkyl nitrates.

189 The total C<sub>9</sub>–C<sub>16</sub> *n*-alkyl nitrate concentrations were 9.67–2730 pg/m<sup>3</sup>, and the mean was 578 pg/m<sup>3</sup>. As  
190 shown in Table 1, the particulate-bound *n*-alkyl nitrate homologue concentration range and mean  
191 increased as the carbon chain length increased. The C<sub>16</sub> *n*-alkyl nitrate homologue had the highest  
192 concentration range, and the mean concentration was significantly higher than the mean concentrations



193 of the other homologues ( $p < 0.01$ ). The  $C_{12}$ – $C_{16}$  *n*-alkyl nitrate concentrations were significantly higher  
194 than the  $C_9$ – $C_{11}$  *n*-alkyl nitrate concentrations ( $p < 0.01$ ), i.e., the long-chain *n*-alkyl nitrate  
195 concentrations were higher than the short-chain *n*-alkyl nitrate concentrations in the  $PM_{2.5}$  samples.

196 The particulate-bound *n*-alkyl nitrate homologue group compositions in the day and night in the  
197 different seasons during the sampling period are shown in Figures 2 and 3. It can be seen that the  $C_{12}$ ,  
198  $C_{14}$ ,  $C_{15}$ , and  $C_{16}$  *n*-alkyl nitrate homologues made relatively high contributions to the total *n*-alkyl  
199 nitrate concentrations and that *n*-alkyl nitrates with longer carbon chains ( $C_{12}$ – $C_{16}$ ) generally  
200 contributed more than *n*-alkyl nitrates with shorter carbon chains ( $C_9$ – $C_{11}$ ) to the total *n*-alkyl nitrate  
201 concentrations during the sampling period.

202 The long-chain *n*-alkyl nitrate concentrations and contributions to the total *n*-alkyl nitrate  
203 concentrations in  $PM_{2.5}$  may have been high because of high concentrations of precursor *n*-alkanes in  
204 the atmosphere and the abilities of *n*-alkyl nitrates to form on airborne particles. *n*-Alkane volatility  
205 decreases as the carbon chain length increases, and long-chain *n*-alkanes are more abundant than  
206 short-chain *n*-alkanes in airborne particulate matter. The alkyl nitrate yield increases as the carbon  
207 chain lengths of the precursor alkanes increase (Lim et al., 2009; Matsunaga et al., 2009; Yeh et al.,  
208 2014). The *n*-alkyl nitrate (monofunctional organic nitrate) stability increases and the saturated vapour  
209 pressure decreases as the carbon chain length increases. Long-chain alkyl nitrates therefore tend more  
210 than short-chain alkyl nitrates to be associated with airborne particles and to be involved in particulate  
211 matter formation (Lim et al., 2005; Yee et al., 2012). The increasing *n*-alkyl nitrate concentrations in  
212 the particulate phase as the *n*-alkyl nitrate carbon chain length increased needed to be investigated  
213 further by investigating the mechanisms involved in *n*-alkyl nitrate formation.

### 214 3.1.2 Diurnal and seasonal variations in *n*-alkyl nitrate concentrations and homologue patterns

215 As shown in Table 1, the mean  $C_9$ – $C_{16}$  *n*-alkyl nitrate concentrations in  $PM_{2.5}$  were higher at night than  
216 in the day and the mean  $C_{12}$ – $C_{16}$  *n*-alkyl nitrate concentrations were significantly higher at night than in  
217 the day ( $p < 0.01$ ). However, the contributions of the different *n*-alkyl nitrates to the total *n*-alkyl nitrate  
218 concentrations in the day and night samples were not significantly different, as shown in Figures 2 and  
219 3. We concluded that the diurnal changes in the particulate-bound *n*-alkyl nitrate concentrations may  
220 have been caused by diurnal changes in meteorological conditions affecting partitioning of the  
221 semi-volatile compounds between the gas and particle phases or by diurnal changes in  
222 particulate-bound alkyl nitrate formation.

223 Temporal trends in the total  $C_9$ – $C_{16}$  *n*-alkyl nitrate concentrations during the sampling period are shown  
224 in Figure 4. The *n*-alkyl nitrate concentrations varied seasonally, with the maximum total concentration  
225 occurring in winter and the mean concentration decreasing in the order winter > spring > autumn >  
226 summer. The contributions of the different *n*-alkyl nitrate homologues varied seasonally, with the  
227 contributions in summer being significantly different from the contributions in the other seasons  
228 ( $p < 0.01$ ) but the compositions in winter, spring, and autumn not being significantly different. The mean  
229 particulate-bound *n*-alkyl nitrate concentrations in winter and spring were significantly higher than the  
230 mean particulate-bound *n*-alkyl nitrate concentrations in summer and autumn ( $p < 0.01$ ). The mean  
231 particulate-bound *n*-alkyl nitrate concentration was lowest in summer even though the maximum  
232 short-chain ( $C_1$ – $C_5$ ) alkyl nitrate concentration in the gas phase was previously found to occur in the  
233 summer (Simpson et al., 2006; Wang et al., 2013; Ling et al., 2016; Sun et al., 2018). We concluded  
234 that long-chain particulate-bound *n*-alkyl nitrates and short-chain alkyl nitrates have different formation  
235 mechanisms.



236 **3.2 Particulate-bound *n*-alkyl nitrate formation mechanisms**

237 **3.2.1 Involvement of particulate-bound *n*-alkyl nitrates in photochemical reactions**

238 It is generally agreed that organic nitrates are secondary products of gas-phase photochemical reactions  
239 in the atmosphere (Perring et al., 2013; Ng et al., 2017) and that organic nitrates enter the particulate  
240 phase through gas–particle partitioning (Capouet et al., 2005; Gu et al., 2017). At high background  
241 NO<sub>x</sub> concentrations, short-chain (C<sub>1</sub>–C<sub>5</sub>) alkyl nitrates are mainly produced through gas-phase  
242 reactions between alkanes and OH· radicals during the day (i.e., in the presence of sunlight) (Robert,  
243 1990; Wisthaler et al., 2008). Alkanes react with OH· radicals to form alkyl radicals through hydrogen  
244 subtraction, and the alkyl radicals are further oxidized to give RO<sub>2</sub>· radicals. Finally, the RO<sub>2</sub>· radicals  
245 react with nitric oxide to give alkyl nitrates. Short-chain (C<sub>1</sub>–C<sub>5</sub>) alkyl nitrates have been found to be  
246 secondary products of photochemical reactions, and short-chain alkyl nitrate concentrations have been  
247 found to correlate with the concentrations of photochemical pollutants and in particular to significantly  
248 positively correlate with the ozone concentration (Wang et al., 2013; Ling et al., 2016; Sun et al., 2018).  
249 Short-chain alkyl nitrate concentrations vary temporally in a similar way to the peroxyacetyl nitrate  
250 concentration, with the maximum concentration occurring in summer (Simpson et al., 2006). However,  
251 the temporal trends in particulate-bound long-chain *n*-alkyl nitrate concentrations we found were  
252 different from the temporal trends in gas-phase short-chain alkyl nitrate concentrations found in  
253 previous studies.

254 Temporal trends in the total C<sub>9</sub>–C<sub>16</sub> *n*-alkyl nitrate concentrations and ozone concentrations during the  
255 sampling period were compared to investigate the relationships between particulate-bound *n*-alkyl  
256 nitrates and photochemical reactions. The C<sub>9</sub>–C<sub>16</sub> *n*-alkyl nitrate and ozone concentrations are shown in  
257 Figure 5. The total particulate-bound *n*-alkyl nitrate and ozone concentrations followed opposite  
258 temporal trends, with the lowest ozone concentration and highest total particulate-bound *n*-alkyl nitrate  
259 concentration occurring in winter and the highest ozone concentration and lowest particulate-bound  
260 *n*-alkyl nitrate concentration occurring in summer. A significant negative correlation was found  
261 between the ozone and particulate-bound *n*-alkyl nitrate concentrations ( $p < 0.01$ ,  $r = -0.411$ ). The C<sub>9</sub>, C<sub>10</sub>,  
262 and C<sub>11</sub> *n*-alkyl nitrate concentrations did not significantly correlate with the ozone concentration but  
263 the C<sub>12</sub>–C<sub>16</sub> *n*-alkyl nitrate concentrations significantly negatively correlated with the ozone  
264 concentration ( $p < 0.01$ ). This and the particulate-bound *n*-alkyl nitrate concentration being higher at  
265 night than in the day suggested that particulate-bound *n*-alkyl nitrates are not indicators of  
266 photochemical pollution and form through different mechanisms from gas-phase short-chain (C<sub>1</sub>–C<sub>5</sub>)  
267 alkyl nitrates. This means that particulate-bound *n*-alkyl nitrates are not formed through photochemical  
268 reactions involving ozone and that long-chain (C<sub>12</sub>–C<sub>16</sub>) *n*-alkyl nitrates are not secondary products of  
269 photochemical reactions.

270 **3.2.2 Possible particulate-bound *n*-alkyl nitrate formation mechanisms**

271 We found that particulate-bound *n*-alkyl nitrates are not products of gas-phase photochemical reactions,  
272 so other mechanisms must be involved in particulate-bound *n*-alkyl nitrate formation. The  
273 particulate-bound *n*-alkyl nitrate and PM<sub>2.5</sub> concentrations significantly correlated ( $p < 0.01$ ,  $r = 0.618$ ) in  
274 a previous study performed in Beijing (Yang et al., 2023). The temporal trends in the particulate-bound  
275 *n*-alkyl nitrate and PM<sub>2.5</sub> concentrations are shown in Figure 6. The C<sub>9</sub>–C<sub>16</sub> *n*-alkyl nitrate and PM<sub>2.5</sub>  
276 concentrations followed similar temporal trends, and the concentrations of both changed synchronously,



277 indicating that the C<sub>9</sub>–C<sub>16</sub> *n*-alkyl nitrate and PM<sub>2.5</sub> concentrations may have correlated. Statistical tests  
278 were performed, and, indeed, a significant positive correlation was found between the  
279 particulate-bound *n*-alkyl nitrate and PM<sub>2.5</sub> concentrations ( $p < 0.01$ ,  $r = 0.664$ ).

280 The particulate-bound C<sub>9</sub>–C<sub>11</sub> *n*-alkyl nitrate homologue concentrations did not significantly correlate  
281 with the PM<sub>2.5</sub> concentration, and the C<sub>9</sub>–C<sub>11</sub> *n*-alkyl nitrates and precursor *n*-alkanes were found at low  
282 detection rates and concentrations in the PM<sub>2.5</sub> samples. We concluded that C<sub>9</sub>–C<sub>11</sub> *n*-alkyl nitrates in  
283 particulate matter may form through both gas-phase and particle-phase reactions. The C<sub>13</sub>–C<sub>16</sub> *n*-alkyl  
284 nitrate homologue concentrations significantly positively correlated with the PM<sub>2.5</sub> concentration  
285 ( $p < 0.01$ ). We concluded that the C<sub>13</sub>–C<sub>16</sub> particulate-bound *n*-alkyl nitrate and particulate matter  
286 concentrations probably correlated because of reactions involving precursors of *n*-alkyl nitrates on the  
287 particulate matter, meaning the particulate matter acted as a medium on which particulate-bound  
288 *n*-alkyl nitrates formed.

289 It has previously been found that organosulfate compounds, which have similar structures to organic  
290 nitrates, can form through non-homogeneous reactions involving sulfate and organosulfate compound  
291 precursors on surfaces of particles (Farmer et al., 2010). Organosulfates and organic nitrates are  
292 important organic pollutants in particulate matter and play important roles in the formation of haze (Li  
293 et al., 2018). Similar compounds may form through similar mechanisms, so we hypothesized that  
294 particulate-bound *n*-alkyl nitrates may form through reactions between alkanes and nitrate on  
295 particulate matter. Semi-volatile *n*-alkanes (precursors of *n*-alkyl nitrates) are widely present in  
296 particulate matter (Kang et al., 2018; Han et al., 2018; Lyu et al., 2019; Yang et al., 2023), and the  
297 *n*-alkane concentration in particulate matter increases as the carbon chain length increases (Aumont et  
298 al., 2012). Abundant *n*-alkanes in particulate matter make it possible for reactions to occur to form  
299 *n*-alkyl nitrates. Nitrogen oxides are precursors of organic nitrates and may be involved in the  
300 formation of particulate-bound *n*-alkyl nitrates, so we compared the temporal trends in the NO<sub>2</sub> and  
301 particulate-bound *n*-alkyl nitrate concentrations. The NO<sub>2</sub> and particulate-bound *n*-alkyl nitrate  
302 concentrations are shown in Figure 7. The C<sub>9</sub>–C<sub>16</sub> particulate-bound *n*-alkyl nitrate and NO<sub>2</sub>  
303 concentrations significantly positively correlated ( $p < 0.01$ ,  $r = 0.626$ ). The C<sub>12</sub>, C<sub>13</sub>, C<sub>14</sub>, C<sub>15</sub>, and C<sub>16</sub>  
304 concentrations significantly positively correlated with the NO<sub>2</sub> concentration ( $p < 0.01$ ), indicating that  
305 NO<sub>2</sub> may be involved in the formation of particulate-bound *n*-alkyl nitrates.

306 It has been found that the formation of nitrate (NO<sub>3</sub><sup>-</sup>) in particulate matter is related to the presence of  
307 NO<sub>2</sub> and that the NO<sub>3</sub><sup>-</sup> and NO<sub>2</sub> concentrations significantly positively correlate (Su et al., 2018). NO<sub>2</sub>  
308 in the atmosphere can be oxidized to NO<sub>3</sub><sup>-</sup> through non-homogeneous reactions on particulate matter  
309 surfaces, and most particulate-phase NO<sub>3</sub><sup>-</sup> forms through these non-homogeneous reactions (Zhu et al.,  
310 2010). The high NO<sub>2</sub> concentrations found in the atmosphere in urban areas mean particulate-phase  
311 nitrate can form. Particulate-bound *n*-alkyl nitrates may form through non-homogeneous reactions  
312 between *n*-alkanes and nitrate on particulate matter surfaces. It has previously been found that  
313 *n*-alkanes can react with nitrate at room temperature with catalysis by metallic copper to give alkyl  
314 nitrates (Luxenhofer et al., 1994; Luxenhofer et al., 1996). Copper is widely present in airborne  
315 particulate matter in urban areas (Duan et al., 2014; Gonzalez et al., 2016) and could catalyse the  
316 formation of particulate-bound *n*-alkyl nitrates. The similar temporal trends in the particulate-bound  
317 *n*-alkyl nitrate, PM<sub>2.5</sub>, and NO<sub>2</sub> concentrations and the significant positive correlations between the  
318 *n*-alkyl nitrate, PM<sub>2.5</sub>, and NO<sub>2</sub> concentrations led us to conclude that particulate-bound *n*-alkyl nitrates  
319 form through reactions between precursor alkanes and particulate-bound nitrate on particulate matter  
320 surfaces.





### 321 3.3 Contributions of particulate-bound *n*-alkyl nitrates to haze pollution

322 The temporal trends in the particulate-bound *n*-alkyl nitrate and PM<sub>2.5</sub> concentrations were similar, as  
323 shown in Figure 6. The particulate-bound *n*-alkyl nitrate and PM<sub>2.5</sub> concentrations significantly  
324 positively correlated ( $p < 0.01$ ,  $r = 0.664$ ), indicating that particulate-bound *n*-alkyl nitrates contributed to  
325 the formation of particulate matter. The particulate-bound *n*-alkyl nitrate and PM<sub>2.5</sub> concentrations  
326 increased sharply during haze pollution events in winter, spring, and autumn, indicating that  
327 particulate-bound *n*-alkyl nitrates are important components of SOAs and make marked contributions  
328 to atmospheric particulate matter and haze. Similar results were found in previous studies of organic  
329 nitrates (Rollins et al., 2012). Changes in the C<sub>9</sub>–C<sub>16</sub> particulate-bound *n*-alkyl nitrate homologue  
330 concentrations during the sampling period are shown in Figure 8. It can be seen that the temporal  
331 changes in the *n*-alkyl nitrate homologue concentrations became more similar to the temporal changes  
332 in the PM<sub>2.5</sub> concentration as the carbon chain length increased. Each C<sub>13</sub>–C<sub>16</sub> *n*-alkyl nitrate  
333 homologue concentration significantly positively correlated with the PM<sub>2.5</sub> concentration ( $p < 0.01$ ), and  
334 the correlation coefficient increased as the *n*-alkyl nitrate carbon chain length increased. This indicated  
335 that the contribution of *n*-alkyl nitrates to the formation of particulate matter and haze increased as the  
336 carbon chain length increased. Because of the high background NO<sub>x</sub> concentration in ambient air in  
337 urban areas, particulate-bound *n*-alkyl nitrate SOAs can make important contributions to the particulate  
338 matter concentration and therefore to haze. Organic nitrates have been found to contribute 2%–12% of  
339 particulate matter in SOAs (Fry et al., 2008; Rollins et al., 2012; Fry et al., 2013; Xu et al., 2015),  
340 meaning that the contributions of organic nitrates to particulate matter in the atmosphere should not be  
341 ignored and that anthropogenic precursors for long-chain particulate-bound *n*-alkyl nitrates are  
342 abundant in the environment and should therefore be of more concern than is currently the case. The  
343 particulate-bound *n*-alkyl nitrate concentration and atmospheric visibility significantly negatively  
344 correlated ( $p < 0.01$ ,  $r = -0.698$ ), indicating that an increase in the particulate-bound *n*-alkyl nitrate  
345 concentration will strongly decrease atmospheric visibility during a haze event. We concluded that  
346 particulate-bound *n*-alkyl nitrates strongly affect haze pollution and that controlling anthropogenic  
347 emissions of NO<sub>x</sub> and VOCs (precursors of particulate-bound *n*-alkyl nitrates) would effectively  
348 control particulate matter pollution and improve air quality in urban areas.

### 349 4 Conclusions

350 The concentrations of *n*-alkyl nitrates in PM<sub>2.5</sub> were determined, and all eight C<sub>9</sub>–C<sub>16</sub> *n*-alkyl nitrate  
351 homologues were detected in PM<sub>2.5</sub>, indicating that long-chain alkyl nitrates are present in airborne  
352 particulate matter in Beijing. The total C<sub>9</sub>–C<sub>16</sub> *n*-alkyl nitrate concentrations during the sampling period  
353 were 9.67–2731.82 pg/m<sup>3</sup>, and the mean was 578.44 pg/m<sup>3</sup>. The detection rate, concentration range,  
354 and mean concentration of each *n*-alkyl nitrate homologue group in the particulate matter samples  
355 increased as the carbon chain length increased. The C<sub>12</sub>–C<sub>16</sub> *n*-alkyl nitrates contributed more than the  
356 C<sub>9</sub>–C<sub>11</sub> *n*-alkyl nitrates to the total *n*-alkyl nitrate concentrations, indicating that long-chain *n*-alkyl  
357 nitrates were more abundant than short-chain *n*-alkyl nitrates in the particulate matter. There were  
358 marked diurnal and seasonal differences in the particulate-bound *n*-alkyl nitrate concentrations. The  
359 mean C<sub>12</sub>–C<sub>16</sub> *n*-alkyl nitrate concentrations were significantly higher at night than in the day ( $p < 0.01$ ).  
360 The maximum particulate-bound *n*-alkyl nitrate concentrations occurred in winter, and the mean  
361 concentrations decreased in the order winter > spring > autumn > summer. The lowest mean  
362 concentration was found in summer even though the maximum short-chain (C<sub>1</sub>–C<sub>5</sub>) alkyl nitrate



363 concentrations in the gas phase has previously been found to occur in summer. The particulate-bound  
364 *n*-alkyl nitrate concentration followed the opposite temporal trend to and significantly negatively  
365 correlated with the ozone concentration. We concluded that long-chain particulate-bound *n*-alkyl  
366 nitrates form through different mechanisms to gas-phase short-chain alkyl nitrates and are not  
367 secondary products of gas-phase photochemical reactions. The particulate-bound *n*-alkyl nitrate  
368 concentration followed the same temporal trend to and significantly positively correlated with the  
369 PM<sub>2.5</sub> and NO<sub>2</sub> concentrations ( $p < 0.01$ ). Particulate-bound *n*-alkyl nitrates may form through  
370 non-homogeneous reactions between alkanes and nitrate on particulate matter surfaces, meaning that  
371 particulate matter acts as a reaction substrate and reactant carrier. Particulate-bound *n*-alkyl nitrates are  
372 important contributors of airborne particulate matter and strongly affect atmospheric visibility, meaning  
373 the roles of particulate-bound *n*-alkyl nitrates in the formation of haze cannot be ignored and  
374 controlling anthropogenic emissions of precursors of particulate-bound *n*-alkyl nitrates in urban areas  
375 with high background NO<sub>x</sub> concentrations will effectively control haze pollution and improve air  
376 quality.

#### 377 **Acknowledgements**

378 This work was supported by the National Natural Science Foundation of China [grant no. 91744206]  
379 and the Beijing Science and Technology Planning Project [Z181100005418016]. We also thank Dr.  
380 Gareth Thomas for his help editing this paper to improve the grammar.

#### 381 **Data availability**

382 The data presented in this article are available from the authors upon request (junjin3799@126.com).

#### 383 **Author contribution**

384 JJ conceived and designed the study, provided direct funding, and helped with manuscript revision.  
385 JYY and GYL mainly conducted the sampling and sample analysis and wrote and revised the  
386 manuscript. The other authors helped with sampling and analysis. All authors read and approved the  
387 final manuscript.

#### 388 **Competing interests**

389 The authors declare that they have no conflict of interest.

#### 390 **References**

391 Aumont, B., Valorso, R., Mouchel-Vallon, C., Camredon, M., Lee-Taylor, J., and Madronich, S.:  
392 Modeling SOA formation from the oxidation of intermediate volatility n-alkanes, *Atmos. Chem. Phys.*,  
393 12, 7577-7589, doi: 10.5194/acp-12-7577-2012, 2012.



- 394 Barnes, I., Becker, K. H., and Zhu, T.: Near UV absorption spectra and photolysis products of  
395 difunctional organic nitrates: Possible importance as NO<sub>x</sub> reservoirs, *J. Atmos. Chem.*, 17, 353-373, doi:  
396 10.1007/BF00696854, 1993.
- 397 Barnes, I., Bastian, V., Becker, K. H., and Zhu, T.: Kinetics and products of the reactions of nitrate  
398 radical with monoalkenes, dialkenes, and monoterpenes, *J. Phys. Chem. C*, 94, 2413-2419, doi:  
399 10.1021/j100369a041, 1990.
- 400 Browne, E. C., and Cohen, R. C.: Effects of biogenic nitrate chemistry on the NO<sub>x</sub> lifetime in remote  
401 continental regions, *Atmos. Chem. Phys.*, 12, 20673-20716, doi: 10.5194/acp-12-11917-2012, 2012.
- 402 Calvert, J. G., and Madronich, S.: Theoretical study of the initial products of the atmospheric oxidation  
403 of hydrocarbons, *J. Geophys. Res. Atmos.*, 92, 2211-2220, doi: 10.1029/JD092iD02p02211, 1987.
- 404 Capouet, M., and Müller, J. F.: A group contribution method for estimating the vapour pressures of  
405  $\alpha$ -pinene oxidation products, *Atmos. Chem. Phys.*, 6, 1455-1467, doi: 10.5194/acp-6-1455-2006, 2006.
- 406 Chen, X. H., Hulbert, D., and Shepson, P. B.: Measurement of the organic nitrate yield from OH  
407 reaction with isoprene, *J. Geophys. Res. Atmos.*, 103, 25563-25568, doi: 10.1029/98JD01483, 1998.
- 408 Duan, J. C., Tan, J. H., Hao, J. M., and Chai, F. H.: Size distribution, characteristics and sources of  
409 heavy metals in haze episod in Beijing, *J. Environ. Sci.*, 26, 189-196, doi:  
410 10.1016/S1001-0742(13)60397-6, 2014.
- 411 Farmer, D. K., Matsunaga, A., Docherty, K. S., Surratt, J. D., Seinfeld, J. H., Ziemann, P. J., and  
412 Jimenez, J. L.: Atmospheric Chemistry Special Feature: Response of an aerosol mass spectrometer to  
413 organonitrates and organosulfates and implications for atmospheric chemistry. *Proc. Natl. Acad. Sci.*  
414 U.S.A., 107, 6670-6675, doi: 10.1073/pnas.0912340107, 2010.
- 415 Fry, J. L., Kiendler-Scharr, A., Rollins, A. W., Wooldridge, P. J., Brown, S.S., Fuchs, H., Dubé, W.,  
416 Mensah, A., Dal Maso, M., Tillmann, R., Dorn, H. P., Brauers, T., and Cohen, R.C.: Organic nitrate and  
417 secondary organic aerosol yield from NO<sub>3</sub> oxidation of  $\beta$ -pinene evaluated using a gas-phase  
418 kinetics/aerosol partitioning model, *Atmos. Chem. Phys.*, 9, 1431-1449, doi: 10.5194/acp-9-1431-2009,  
419 2009.
- 420 Fry, J. L., Draper, D. C., Zarzana, K. J., Campuzano-Jost, P., Day, D. A., Jimenez, J. L., Brown, S. S.,  
421 Cohen, R. C., Kaser, L., Hansel, A., Cappellin, L., Karl, T., Hodzic Roux, A., Turnipseed, A., Cantrell,  
422 C., Lefer, B. L., and Grossberg, N.: Observations of gas- and aerosol-phase organic nitrates at  
423 BEACHON-RoMBAS 2011, *Atmos. Chem. Phys.*, 13, 8585-8605, doi: 10.5194/acp-13-8585-2013,  
424 2013.
- 425 Garnes, L. A., and Allen, D. T.: Size Distributions of Organonitrates in Ambient Aerosol Collected in  
426 Houston, Texas. *Aerosol Sci. Technol.*, 36, 983-992, doi: 10.1080/02786820290092186, 2002.
- 427 Gonzalez, R. O., Strekopytov, S., Amato, F., Querol, X., Reche, C., and Weiss, D.: New insights from  
428 zinc and copper isotopic compositions into the sources of atmospheric particulate matter from two  
429 major European cities, *Environ. Sci. Technol.*, 50, 9816-9824, doi: 10.1021/acs.est.6b00863, 2016.
- 430 Gu, F. T., Hu, M., Zheng, J., and Guo, S.: Research Progress on Particulate Organonitrates, *Prog. Chem.*  
431 (in Chinese), 29, 962-969, doi: 10.7536/PC170324, 2017.
- 432 Han, D. M., Fu, Q. Y., Gao, S., Li, L., Ma, Y. G., Qiao, L. P., Xu, H., Liang, S., Cheng, P. F., Chen, X.  
433 J., Zhou, Y., Yu, J. Z., and Chen, J. P.: Non-polar organic compounds in autumn and winter aerosols in a



434 typical city of eastern China: size distribution and impact of gas-particle partitioning on PM<sub>2.5</sub> source  
435 apportionment, *Atmos. Chem. Phys.*, 18, 9375-9391, doi: 10.5194/acp-18-9375-2018, 2018.

436 Jordan, C. E., Ziemann, P. J., Griffin, R. J., Lim, Y. B., Atkinson, R., Arey, J.: Modeling SOA formation  
437 from OH reactions with C<sub>8</sub>-C<sub>17</sub> n-alkanes, *Atmos. Environ.*, 42, 8015-8026, doi:  
438 10.1016/j.atmosenv.2008.06.017, 2008.

439 Kang, M. J., Fu P. Q., Aggarwal, S. G., Kumar, S., Zhao, Y., Sun, Y. L., and Wang, Z. F.: Size  
440 distributions of n-alkanes, fatty acids and fatty alcohols in springtime aerosols from New Delhi, India,  
441 *Environ. Pollut.*, 219, 957-966, doi: 10.1016/j.envpol.2016.09.077, 2016.

442 Li, H., Zhang, Q., Zheng, B., Chen, C., Wu, N., Guo, H., Zhang, Y., Zheng, Y., Li, X., and He, K.:  
443 Nitrate-driven urban haze pollution during summertime over the North China Plain, *Atmos. Chem.*  
444 *Phys.*, 18, 5293-5306, doi: 10.5194/acp-18-5293-2018, 2018.

445 Lim, Y. B., and Ziemann, P. J.: Products and Mechanism of Secondary Organic Aerosol Formation  
446 from Reactions of n-Alkanes with OH Radicals in the Presence of NO<sub>x</sub>. *Environ. Sci. Technol.*, 39,  
447 9229-9236, doi: 10.1021/es051447g, 2005.

448 Lim, Y. B., and Ziemann, P. J.: Chemistry of Secondary Organic Aerosol Formation from OH  
449 Radical-Initiated Reactions of Linear, Branched, and Cyclic Alkanes in the Presence of NO<sub>x</sub>. *Aerosol*  
450 *Sci. Technol.*, 43, 604-619, doi: 10.1080/02786820902802567, 2009.

451 Ling, Z., Guo, H., Simpson, I. J., Saunders, S. M., Lam, S. H. M., Lyu, X., and Blake, D. R.: New  
452 insight into the spatiotemporal variability and source apportionments of C<sub>1</sub>-C<sub>4</sub> alkyl nitrates in Hong  
453 Kong, *Atmos. Chem. Phys.*, 16, 8141-8156, <https://doi.org/10.5194/acp-16-8141-2016>, 2016.

454 Liu, X. J., Zhang, Y., Han, W. X., Tang, A. H., Shen, J. L., Cui, Z. L., Vitousek, P., Erisman, J. W.,  
455 Goulding, K., Christie, P., Fangmeier, A., and Zhang, F. S.: Enhanced nitrogen deposition over China,  
456 *Nature*, 494, 458-463, doi: 10.1038/nature11917, 2013.

457 Liu, Y. and Wang, T.: Worsening urban ozone pollution in China from 2013 to 2017 - Part 2: The  
458 effects of emission changes and implications for multi-pollutant control, *Atmos. Chem. Phys.*, 20,  
459 6323-6337, doi: 10.5194/acp-20-6323-2020, 2020.

460 Luxenhofer, O., Schneider, E., and Ballschmiter, K.: Separation, detection and occurrence  
461 of (C<sub>2</sub>-C<sub>8</sub>)-alkyl- and phenyl-alkyl nitrates as trace compounds in clean and polluted air, *Fresenius J.*  
462 *Anal. Chem.*, 350, 384-394, doi: 10.1007/BF00325611, 1994.

463 Luxenhofer, O., Schneider, M., Dambach, M. and Ballschmiter, K.: Semivolatile long chain C<sub>6</sub>-C<sub>17</sub>  
464 alkyl nitrates as trace compounds in air, *Chemosphere*, 33, 393-404, doi:  
465 10.1016/0045-6535(96)00205-6, 1996.

466 Lyu, R. H., Shi, Z. B., Alam, M. S., Wu, X. F., Liu, D., Vu, T. V, Stark, C., Xu, R. X., Fu, P. Q., Feng, Y.  
467 C., and Harrison, R. M: Alkanes and aliphatic carbonyl compounds in wintertime PM 2.5 in Beijing,  
468 China, *Atmos. Environ.*, 202, 244-255, doi: 10.1016/j.atmosenv.2019.01.023, 2019.

469 Ma, J. Z., Xu, X. B., Zhao, C. S., and Yan, P.: A review of atmospheric chemistry research in China:  
470 Photochemical smog, haze pollution, and gas-aerosol interactions, *Adv. Atmos. Sci.*, 29, 1006-1026,  
471 doi: 10.1007/s00376-012-1188-7, 2012.

472 Matsunaga, A., Ziemann, P. J.: Yields of beta-hydroxynitrates and dihydroxynitrates in aerosol formed  
473 from OH radical-initiated reactions of linear alkenes in the presence of NO<sub>x</sub>, *J. Phys. Chem. A*, 113,



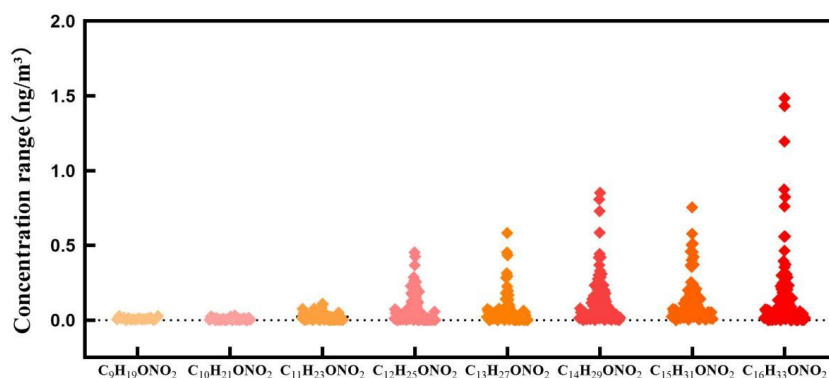
- 474 599-606, doi: 10.1021/jp807764d, 2009.
- 475 Mijling, B., van der A, R. J., and Zhang, Q.: Regional nitrogen oxides emission trends in East Asia  
476 observed from space, *Atmos. Chem. Phys.*, 13, 12003-12012, doi: 10.5194/acp-13-12003-2013, 2013.
- 477 Ng, N. L., Brown, S. S., Archibald, A. T., Atlas, E., Cohen, R. C., Crowley, J. N., Day, D. A., Donahue,  
478 N. M., Fry, J. L., Fuchs, H., Griffin, R. J., Guzman, M. I., Herrmann, H., Hodzic, A., Iinuma, Y.,  
479 Jimenez, J. L., Kiendler-Scharr, A., Lee, B. H., Luecken, D. J., Mao, J., McLaren, R., Mutzel, A.,  
480 Osthoff, H. D., Ouyang, B., Picquet-Varrault, B., Platt, U., Pye, H. O. T., Rudich, Y., Schwantes, R. H.,  
481 Shiraiwa, M., Stutz, J., Thornton, J. A., Tilgner, A., Williams, B. J., and Zaveri, R. A.: Nitrate radicals  
482 and biogenic volatile organic compounds: oxidation, mechanisms, and organic aerosol, *Atmos. Chem.*  
483 *Phys.*, 17, 2103-2162, doi: 10.5194/acp-17-2103-2017, 2017.
- 484 Perring, A. E., Wisthaler, A., Graus, M., Wooldridge, P. J., Lockwood, A. L., Mielke, L. H., Shepson, P.  
485 B., Hansel, A., and Cohen, R. C.: A product study of the isoprene+NO<sub>3</sub> reaction, *Atmos. Chem. Phys.*,  
486 9, 4945-4956, doi: 10.5194/acp-9-4945-2009, 2009.
- 487 Perring, A. E., Bertram, T. H., Farmer, D. K., Wooldridge, P. J., Dibb, J., Blake, N. J., Blake, D. R.,  
488 Singh, H. B., Fuelberg, H., Diskin, G., Sachse, G., and Cohen, R. C.: The production and persistence of  
489 ΣRONO<sub>2</sub> in the Mexico City plume, *Atmos. Chem. Phys.*, 10, 7215-7229, doi:  
490 10.5194/acp-10-7215-2010, 2010.
- 491 Perring, A. E., Pusede, S. E., and Cohen, R. C.: An observational perspective on the atmospheric  
492 impacts of alkyl and multifunctional nitrates on ozone and secondary organic aerosol, *Chem. Rev.*, 113,  
493 5848-5870, doi: 10.1021/cr300520x, 2013.
- 494 Richter, A., Burrows, J. P., Nub, H., Granier, C., and Niemeier, U.: Increase in tropospheric nitrogen  
495 dioxide over China observed from space, *Nature*, 437, 129-132, doi: 10.1038/nature04092, 2005.
- 496 Rindelaub, J. D., Mcavey, K. M., and Shepson, P. B.: The photochemical production of organic nitrates  
497 from α-pinene and loss via acid-dependent particle phase hydrolysis, *Atmos. Environ.*, 100, 193-201,  
498 doi: 10.1016/j.atmosenv.2014.11.010, 2015.
- 499 Roberts, J. M.: The atmospheric chemistry of organic nitrates. *Atmos. Environ.*, 24, 243-287, doi:  
500 10.1016/0960-1686(90)90108-Y, 1990.
- 501 Rollins, A. W., Kiendler-Scharr, A., Fry, J. L., Brauers, T., Brown, S. S., Dorn, H.-P., Dubé, W. P.,  
502 Fuchs, H., Mensah, A., Mentel, T. F., Rohrer, F., Tillmann, R., Wegener, R., Wooldridge, P. J., and  
503 Cohen, R. C.: Isoprene oxidation by nitrate radical: alkyl nitrate and secondary organic aerosol yields,  
504 *Atmos. Chem. Phys.*, 9, 6685-6703, doi: 10.5194/acp-9-6685-2009, 2009.
- 505 Rollins, A. W., Browne, E. C., Min, K. E., Pusede, S. E., Wooldridge, P. J., Gentner, D. R., Goldstein, A.  
506 H., Liu, S., Day, D. A., Russell, L. M.: Evidence for NO<sub>x</sub> Control over Nighttime SOA Formation,  
507 *Science*, 337, 1210-1212, doi: 10.1126/science.1221520, 2012.
- 508 Shen, H. R., Zhao, D. F., Pullinen, L., Kang, S., Vereecken, L., Fuchs, L., Acir, I. H., Tillmann, R.,  
509 Rohrer, f., Wildt, J.: Highly Oxygenated Organic Nitrates Formed from NO<sub>3</sub> Radical-Initiated  
510 Oxidation of β-Pinene, *Environ. Sci. Technol.*, 55, 15658-15671, doi: 10.1021/acs.est.1c03978, 2021.
- 511 Simpson, I. J., Wang, T., Guo, H., Kwok, Y. H., Flocke, F., Atlas, E., Meinardi, S., Rowland, F. S., and  
512 Blake, D. R.: Long-term atmospheric measurements of C<sub>1</sub>-C<sub>5</sub> alkyl nitrates in the Pearl River Delta  
513 region of southeast China, *Atmos. Environ.*, 40, 1619-1632, doi: 10.1016/j.atmosenv.2005.10.062



- 514 2006.
- 515 Spittler, M., Barnes, I., Bejan, I., Brockmann, K. J., Benter, T., and Wirtz, K.: Reactions of NO<sub>3</sub>  
516 radicals with limonene and  $\alpha$ -pinene: Product and SOA formation, *Atmos. Environ.*, 40, 116-127, doi:  
517 10.1016/j.atmosenv.2005.09.093, 2006.
- 518 Su, J., Zhao, P., and Dong, Q.: Chemical compositions and liquid water content of size-resolved aerosol  
519 in Beijing, *Aerosol Air Qual. Res.*, 18, 680-692, doi: 10.4209/aaqr.2017.03.0122, 2018.
- 520 Sun, J., Li, Z., Xue, L., Wang, T., Wang, X., Gao, J., Nie, W., Simpson, I. J., Gao, R., and Blake, D. R.:  
521 Summertime C1-C5 alkyl nitrates over Beijing, northern China: Spatial distribution, regional transport,  
522 and formation mechanisms, *Atmos. Res.*, 204, 102-109, doi: 10.1016/j.atmosres.2018.01.014, 2018.
- 523 Sun, Y. L., Zhang, Q., Schwab, J. J., Yang, T., Ng, N. L., and Demerjian, K. L.: Factor analysis of  
524 combined organic and inorganic aerosol mass spectra from high resolution aerosol mass spectrometer  
525 measurements, *Atmos. Chem. Phys.*, 12, 8537-8551, doi:10.5194/acp-12-8537-2012, 2012.
- 526 Vasquez, K. T., Crounse, J. D., Schulze, B. C., Bates, K. H., Wennberg, P. O.: Rapid hydrolysis of  
527 tertiary isoprene nitrate efficiently removes NO<sub>x</sub> from the atmosphere. *Proc. Natl. Acad. Sci. U.S.A.*,  
528 117, 33011-33016, doi: 10.1073/pnas.2017442117, 2020.
- 529 Wang, M., Shao, M., Chen, W., Lu, S., Wang, C., Huang, D., Yuan, B., Zeng, L., and Zhao, Y.:  
530 Measurements of C1-C4 alkyl nitrates and their relationships with carbonyl compounds and O<sub>3</sub> in  
531 Chinese cities, *Atmos. Environ.*, 81, 389-398, doi: 10.1016/j.atmosenv.2013.08.065, 2013.
- 532 Wei, W., Li, Y., Wang, Y., Cheng, S., and Wang, L.: Characteristics of VOCs during haze and non-haze  
533 days in Beijing, China: Concentration, chemical degradation and regional transport impact. *Atmos.*  
534 *Environ.*, 194, 134-145, doi: 10.1016/j.atmosenv.2018.09.037, 2018.
- 535 Wisthaler, A., Apel, E. C., Bossmeyer, J., Hansel, A., Junkermann, W., Koppmann, R., Meier, R.,  
536 Müller, K., Solomon, S. J., Steinbrecher, R., Tillmann, R., and Brauers, T.: Technical Note:  
537 Intercomparison of formaldehyde measurements at the atmosphere simulation chamber SAPHIR,  
538 *Atmos. Chem. Phys.*, 8, 2189-2200, doi: 10.5194/acp-8-2189-2008, 2008.
- 539 Wu, R., Vereecken, L., Tsiligiannis, E., Kang, S., Albrecht, S. R., Hantschke, L., Zhao, D., Novelli, A.,  
540 Fuchs, H., Tillmann, R., Hohaus, T., Carlsson, P. T. M., Shenolikar, J., Bernard, F., Crowley, J. N., Fry,  
541 J. L., Brownwood, B., Thornton, J. A., Brown, S. S., Kiendler-Scharr, A., Wahner, A., Hallquist, M.,  
542 and Mentel, T. F.: Molecular composition and volatility of multi-generation products formed from  
543 isoprene oxidation by nitrate radical, *Atmos. Chem. Phys.*, 21, 10799-10824, doi:  
544 10.5194/acp-21-10799-2021, 2021.
- 545 Xu, L., Suresh, S., Guo, H., Weber, R. J., and Ng, N. L.: Aerosol characterization over the southeastern  
546 United States using high-resolution aerosol mass spectrometry: spatial and seasonal variation of aerosol  
547 composition and sources with a focus on organic nitrates, *Atmos. Chem. Phys.*, 15, 7307-7336, doi:  
548 10.5194/acp-15-7307-2015, 2015.
- 549 Yang, X. H., Luo, F. X., Li, J. Q., Chen, D. Y., E, Y., Lin, W. L., and Jun, J.: Alkyl and aromatic nitrates  
550 in atmospheric particles determined by gas chromatography tandem mass spectrometry. *J. Am. Soc.*  
551 *Mass. Spectrom.*, 30, 2762-2770, doi: 10.1007/s13361-019-02347-8, 2019.
- 552 Yang, J., Lei, G., Liu, C., Wu, Y., Hu, K., Zhu, J., Bao, J., Lin, W., and Jin, J.: Characteristics of  
553 particulate-bound n-alkanes indicating sources of PM<sub>2.5</sub> in Beijing, China, *Atmos. Chem. Phys.*, 23,

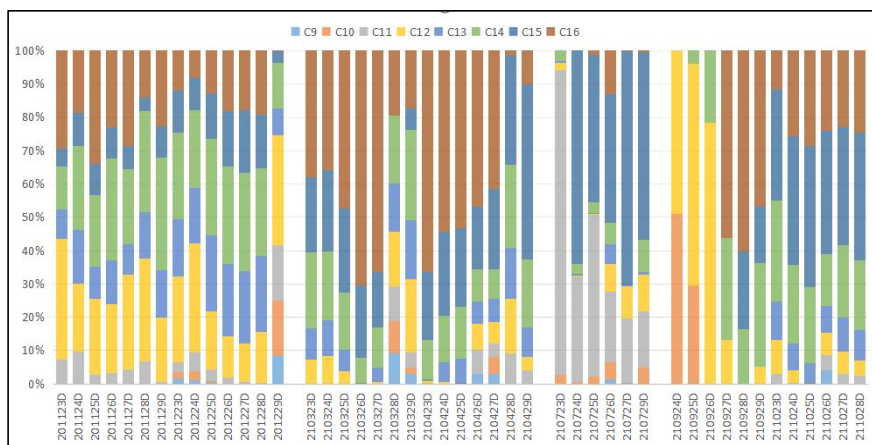


554 3015-3029, doi: 10.5194/acp-23-3015-2023, 2023.  
555 Yang, J., Lei, G., Liu, C., Wu, Y., Hu, K., Zhu, J., Bao, J., Lin, W., and Jin, J.: Characteristics of  
556 particulate-bound n-alkanes indicating sources of PM2.5 in Beijing, China, *Atmos. Chem. Phys.*, 23,  
557 3015–3029, doi: 10.5194/acp-23-3015-2023, 2023.  
558 Yee, L. D., Craven, J. S., Loza, C. L., Schilling, K. A., Ng, N. L., Canagaratna, M. R., Ziemann, P. J.,  
559 Flagan, R. C., and Seinfeld, J. H.: Secondary Organic Aerosol Formation from Low-NOx  
560 Photooxidation of Dodecane: Evolution of Multigeneration Gas-Phase Chemistry and Aerosol  
561 Composition, *J. Phys. Chem. A*, 116, 6211-6230, doi: 10.1021/jp211531h, 2012.  
562 Yeh, G. K., and Ziemann, P. J.: Identification and yields of 1,4-hydroxynitrates formed from the  
563 reactions of C8-C16 n-alkanes with OH radicals in the presence of NOx, *J. Phys. Chem. A*, 118,  
564 8797-8806, doi: 10.1021/jp505870d, 2014.  
565 Zhai, T. Y., Lu, K. D., Wang, H. C., Luo, S. R., Chen, X. R., Hu, R. Z., and Zhang, Y. H.: Elucidate the  
566 formation mechanism of particulate nitrate based on direct radical observations in the Yangtze River  
567 Delta summer 2019, *Atmos. Chem. Phys.*, 23, 2379-2391, doi: 10.5194/acp-23-2379-2023, 2023.  
568 Zhu, T., Shang, J., and Zhao, D. F.: The roles of heterogeneous chemical processes in the formation of  
569 an air pollution complex and gray haze, *Sci. China Chem.*, 40, 1731-1740, doi:  
570 10.1360/zb2010-40-12-1731, 2010.



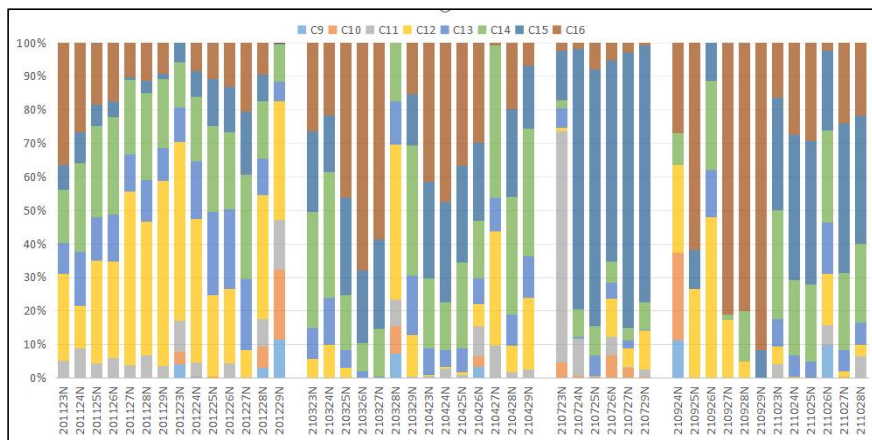
571

572 **Figure 1. Concentrations of C<sub>9</sub>–C<sub>16</sub> n-alkyl nitrates found during the sampling period**



573

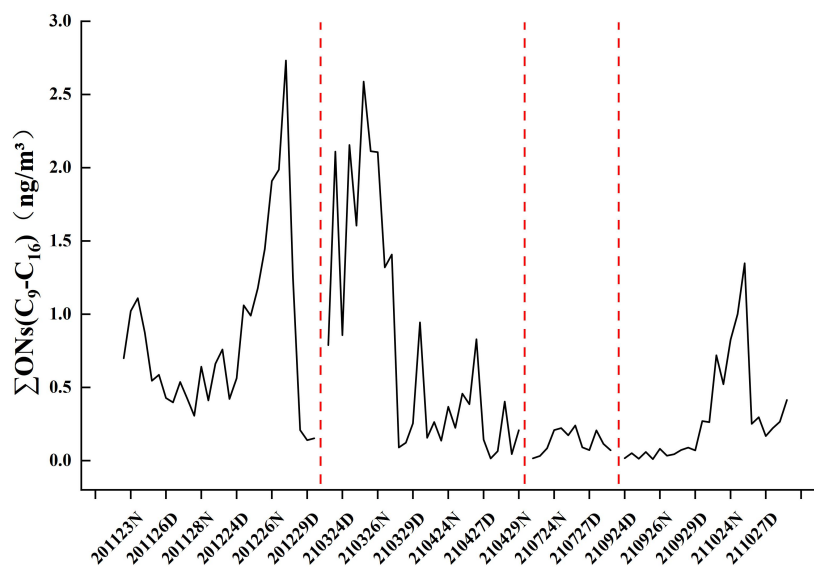
574 **Figure 2. Contributions of the C<sub>9</sub>–C<sub>16</sub> *n*-alkyl nitrate homologues to the total C<sub>9</sub>–C<sub>16</sub> *n*-alkyl nitrate**  
575 **concentrations in the day samples collected in different seasons**



576

577 **Figure 3. Contributions of the C<sub>9</sub>–C<sub>16</sub> *n*-alkyl nitrate homologues to the total C<sub>9</sub>–C<sub>16</sub> *n*-alkyl nitrate**  
578 **concentrations in the night samples collected in different seasons**

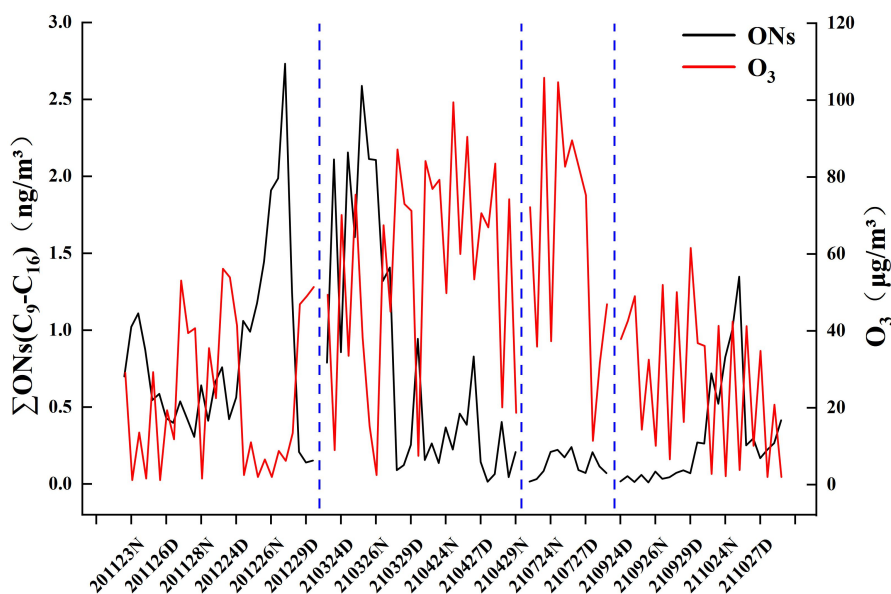




579

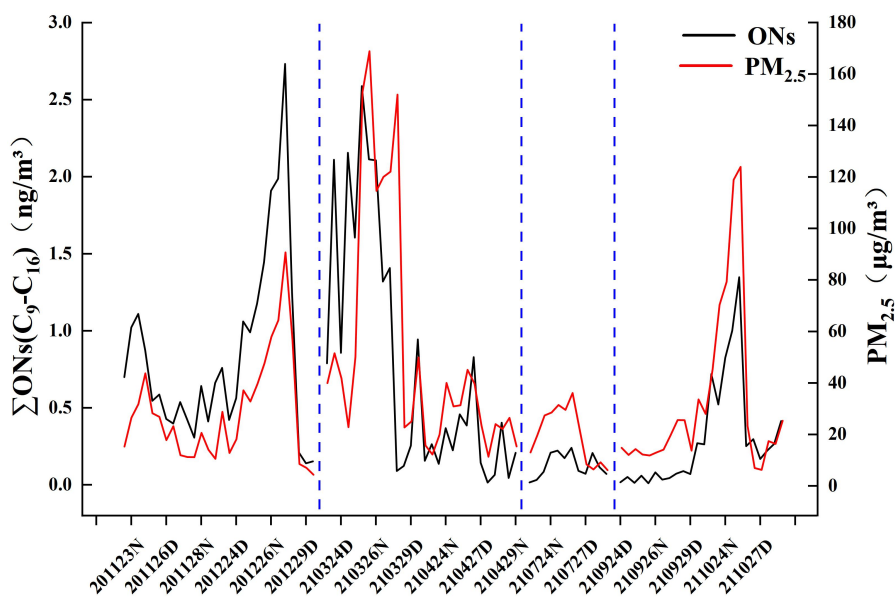
580 Figure 4. Total C<sub>9</sub>-C<sub>16</sub> *n*-alkyl nitrate concentrations during the sampling period

581 (“D” indicates samples collected in the day and “N” indicates samples collected at night)



582

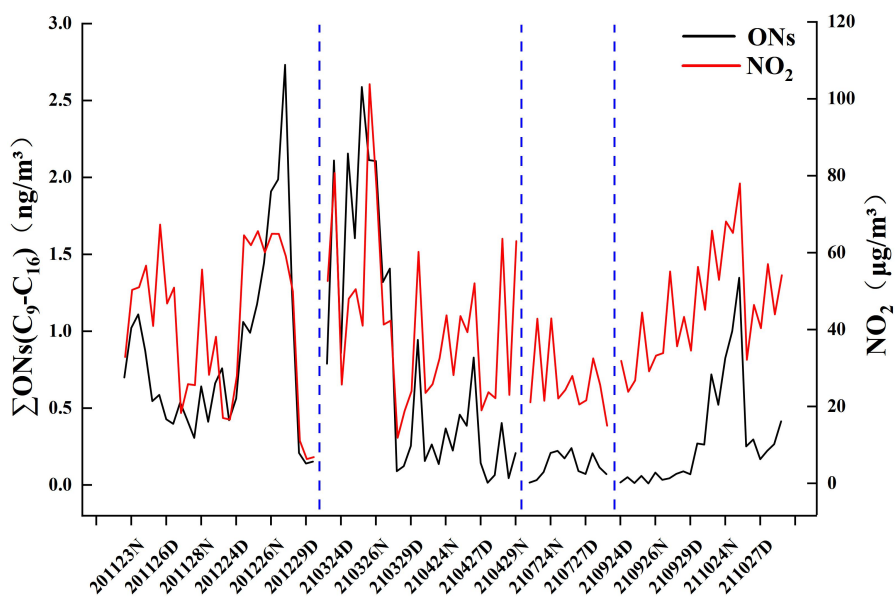
583 Table 5. Total C<sub>9</sub>-C<sub>16</sub> *n*-alkyl nitrate and ozone concentrations



584

585

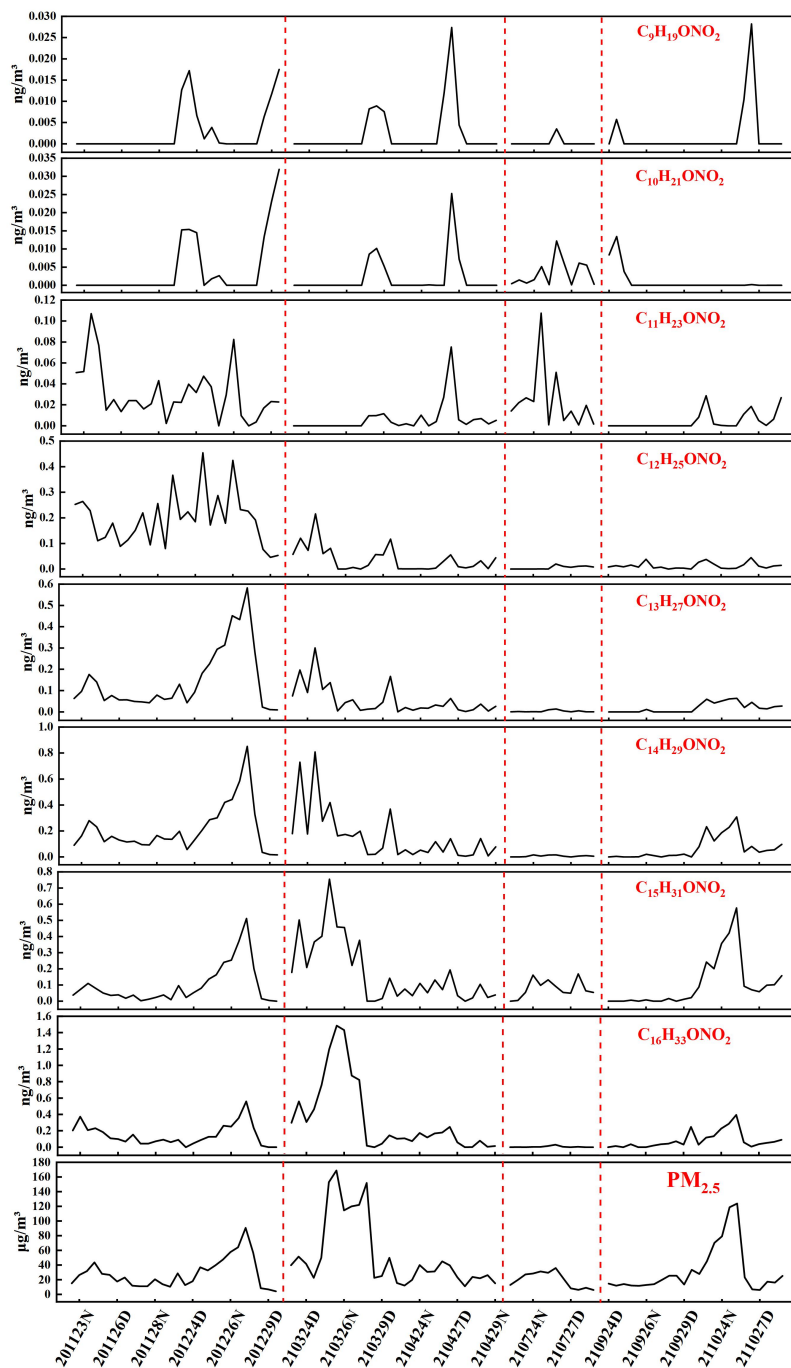
Table 6. Total C<sub>9</sub>–C<sub>16</sub> *n*-alkyl nitrate and PM<sub>2.5</sub> concentrations



586

587

Figure 7. Total C<sub>9</sub>–C<sub>16</sub> *n*-alkyl nitrate and NO<sub>2</sub> concentrations



588

589 **Figure 8.** C<sub>9</sub>–C<sub>16</sub> *n*-alkyl nitrate homologue and PM<sub>2.5</sub> concentrations

590 **Table 1.** C<sub>9</sub>–C<sub>16</sub> *n*-alkyl nitrate concentration ranges, mean concentrations, and detection rates



n-Alkyl nitrates	Concentration range (pg/m <sup>3</sup> )			Mean concentration (pg/m <sup>3</sup> )			Detection rate		
	Day (n=46)	Night (n=46)	Total (n=92)	Day	Night	Total	Day	Night	Total
C <sub>9</sub> H <sub>19</sub> ONO <sub>2</sub>	ND-12.70	ND-28.23	ND-28.23	1.76	2.45	2.11	21.74%	19.57%	20.65%
C <sub>10</sub> H <sub>21</sub> ONO <sub>2</sub>	ND-23.13	ND-31.95	ND-31.95	2.44	2.79	2.61	34.78%	30.43%	32.61%
C <sub>11</sub> H <sub>23</sub> ONO <sub>2</sub>	ND-107.59	ND-82.41	ND-107.59	15.60	15.54	15.57	69.57%	69.57%	69.57%
C <sub>12</sub> H <sub>25</sub> ONO <sub>2</sub>	ND-252.57	ND-454.04	ND-454.04	58.75	91.55	75.15	93.78%	91.30%	92.39%
C <sub>13</sub> H <sub>27</sub> ONO <sub>2</sub>	ND-433.38	ND-582.25	ND-582.25	57.89	76.30	67.10	86.96%	89.13%	88.04%
C <sub>14</sub> H <sub>29</sub> ONO <sub>2</sub>	ND-585.96	ND-851.84	ND-851.84	103.93	159.66	131.79	95.65%	95.65%	95.65%
C <sub>15</sub> H <sub>31</sub> ONO <sub>2</sub>	ND-459.60	ND-755.01	ND-755.01	98.74	145.13	121.94	86.96%	89.13%	88.04%
C <sub>16</sub> H <sub>33</sub> ONO <sub>2</sub>	ND-1485.93	ND-1431.79	ND-1485.93	155.98	190.06	173.02	89.13%	95.65%	92.39%
ΣC <sub>9</sub> -C <sub>16</sub>	9.67-2112.80	14.64-2731.82	9.67-2731.82	495.09	683.48	589.29	100%	100%	100%

591